RSC Advances

ROYAL SOCIETY OF CHEMISTRY

www.rsc.org/advances

The change of tribological behavior of zinc coatings with the reduction of grain size from micro to nano-scales is investigated.

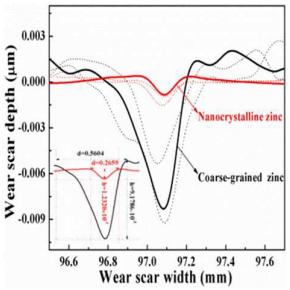

Journal Name

RSCPublishing

ARTICLE

Research on the tribological behavior of nanocrystalline zinc coating prepared by pulse reverse electrodeposition

Cite this: DOI: 10.1039/x0xx00000x

Received 00th January 2012,
Accepted 00th January 2012

DOI: 10.1039/x0xx00000x

www.rsc.org/

Qingyang Li,[a] Zhongbao Feng,[a] Lihua Liu,[b] Jie Sun,[b] Yunteng Qu,[a] Fenghuan Li[a] and Maozhong An[a,*]

Nanocrystalline zinc coatings are electrodeposited by direct current (DC), pulse current (PC) and pulse reverse current (PRC) techniques in a sulfate bath with polyacrylamide as the only additive and are characterized by field-emission scanning electron microscope (FESEM), atomic force microscope (AFM) and X-ray diffraction (XRD). In addition, the influences of current waveforms on grain size, surface roughness and crystallographic preferred orientation of the coatings are analyzed. Specially, the tribological behavior of nanocrystalline and coarse-grained zinc coatings is investigated by nanoindentation, ball-on-disc friction test, profilometer, FESEM and energy dispersive X-ray spectroscopy (EDS). The results show that PRC electrodeposition of nanocrystalline zinc coating has significant advantages in control of the grain size and surface roughness of the coating than DC and PC electrodeposition. The hardness of nanocrystalline zinc coating produced by PRC electrodeposition is almost three times that of the coarse-grained counterpart. And the average wear rate of the nanocrystalline zinc coating is approximately 1/24 of that of the coarse-grained zinc coating. The friction and wear mechanism of zinc coatings experiences transition from severe adhesion and abrasion wear (coarse-grained zinc) to a slight abrasion and oxidation wear (nanocrystalline zinc) with the reduction of grain size.

Introduction

The electrodeposition of zinc has obtained widespread application in mechanical, aerospace, automotive and construction fields because of its impressive performances such as uniform, smooth surface with no defects (crack, burrs, porosity, *etc*.) and good corrosion resistance property. The low cost and simplicity of zinc also make the electrodeposition of a zinc coating an indispensable surface protection technique to the steel nowadays. Although there are many excellent properties, the conventional electrodeposition process (coarse-grain zinc coating) does not alter the structure and properties (mechanical and tribological) of zinc. Therefore, there is a large amount of zinc loss in production and application process caused by the friction and wear between coatings and the environment. Moreover, the poor wear resistance property of the conventional coarse-grained zinc coating also increases the probability of damage and thus, reduces the life of coating. Hence, the coating must be thick enough to endure the attack of a friction and wear environment. However, thick coatings can lead to a waste of zinc, as well as poor weldability, and difficulty to achieve a specular finish after painting, which greatly limits its applications. It therefore needs to develop thinner electrodeposited coatings with improved properties such as hardness, friction and wear, *etc*.[1-3]

Nanocrystalline electrodeposit has exhibited many unusual mechanical, physical, chemical and electrochemical properties due to its grain size below 100nm and high-volume fraction of the grain boundary.[4] Previous researches have demonstrated that the nanocrystalline coatings possess excellent wear resistance,[5,6] corrosion resistance,[7,8] ductility,[9,10] hardness[11,12] and electrochemical properties[13] compared with conventional coarse-grained zinc coatings. The friction and wear behavior of coarse-grained zinc coatings with different grain sizes from 90 to 150 μm have been investigated by Panagopoulos *et al*.[14] The result shows that the wear resistance of zinc increases with decreasing grain size. On the other hand, Saber *et al*.[15] also reported that the microhardness increased to

approximately 5-8 times higher than that when the grain size of coarse-grained zinc coatings was reduced from micro to nano scales (56 nm). And the hardness has played a crucial role in the protection of coatings against the wear.[16,17] Based on above results, the electrodeposition of nanocrystalline zinc coatings becomes a reasonable way to overcome the poor wear resistance of conventional coarse-grained zinc coatings.

So far, most research works have focused on the electrochemical corrosion behavior of nanocrystalline zinc coatings.[18-22] The tribological behavior of nanocrystalline zinc coating has been scarcely studied to date. In our previous work,[23] the nanocrystalline zinc coatings were produced by pulse reverse electrodeposition from a sulfate bath containing polyacrylamide as the only additive, and it was found that the surface nanocrystallization can effectively decrease the friction coefficients of zinc coatings. For this paper, the influences of current waveform on the morphology, crystalline texture and grain size of the nanocrystalline zinc coatings are analysed, and the friction and wear properties of zinc coatings are more systematically investigated through the nanohardness, friction coefficient, wear rate, morphology and elemental composition of worn scar measurements. Specially, interests are focused on the change of tribological behavior of zinc coatings with the reduction of grain size.

Experimental

Preparation and characterization of nanocrystalline zinc coatings

The nanocrystalline zinc coatings were produced by DC, PC and PRC electrodeposition from a sulfate electrolyte with polyacrylamide as the only additive. The electrodeposition bath was made of 100 g L^{-1} of $ZnSO_4 \cdot 7H_2O$ and 20 g L^{-1} of H_3BO_3 with or without the additive, maintained at 23 ± 2 ℃, and agitated slowly by a magnetic stirrer. The pH value of the bath was adjusted to 1-2 by the addition of dilute sulphuric acid. The nonionic type polyacrylamide (1 g L^{-1}) with mean molecular weight 2 000 000~14 000 000 g mol^{-1} was used as the grain refiner. The electrodeposition parameters are listed in Table 1, and a detailed discussion of the experimental procedure is given elsewhere.[23,27] Zinc electrodeposition was carried out in a two-electrode cell containing a 200 mL sulfate bath. The used substrates were steel sheets of 4×4 cm^2 area, which were pretreated by immersion in a solution of 10% sulfuric acid at room temperature for 10 s, and rinsed with distilled water. All electrodeposited samples used flat materials in order to enhance the accuracy of friction and wear testing results. A zinc plate of 99.99% purity was used as the anode. After electrodeposition, the zinc coatings were rinsed immediately in de-ionized water, then dried and subjected directly to characterization and property measurements. All electrodeposition experiments were duplicated and good reproducibility was obtained.

Surface and cross-sectional morphologies of the nanocrystalline zinc coatings were characterized using a field-emission scanning electron microscope (FESEM, Helios Nanolab 600i) with energy dispersive X-ray spectroscopy (EDS). Atomic force microscope (AFM, Bruker Multimode 8) working in the intermittent contact mode was used to examine the surface roughness of coatings. X-ray diffraction (XRD, Rigaku Corporation Dmax-3B) was carried out using Cu Ka radiation in order to determine the crystalline texture, crystallographic preferred orientation and approximate average grain size of the coatings. The grain size was calculated by the Scherrer's formula according to equation (1).

$$D = \frac{K\lambda}{\beta \cos\theta} \quad (1)$$

Where D is the grain size (in nm), K is a constant (0.89), λ is the X-ray wavelength (0.154 nm), β is the full width at half maxima in 2θ degrees, and θ is the diffraction angle.[24]

Table 1 Process parameters for electrodeposition of nanocrystalline zinc coatings.

Electrodeposition parameters	Range
Direct current (DC) electrodeposition	
Current density	3 A dm^{-2}
Time	30 min
Pulse current (PC) electrodeposition	
Pulse current density	3 A dm^{-2}
Duty cycle	20 %
Time	30 min
Pulse reverse current (PRC) electrodeposition	
Forward pulse current density	3 A dm^{-2}
Reverse pulse current density	0.3 A dm^{-2}
Forward pulse durations	100 ms
Reverse pulse durations	10 ms
Duty cycle	20 %
Time	30 min

Tribological behavior of nanocrystalline zinc coatings

The tribolobical behavior of nanocrystalline and coarse-grained zinc coatings was evaluated by hardness, friction coefficients and wear rates, respectively. The hardness values of coatings were evaluated based on load-depth curves obtained by nanoindentation tests (nanoindenter XP, MTS Systems Corporation). All measurements were made at a 1 μm penetration depth with a Berkovich diamond indenter. Typically, 5 indents were obtained for individual specimens, from which the average values were calculated. Friction and wear experiments of the coatings were tested on a ball-on-disk tribometer (Center for Tribology, HIT, China) with a 52100 steel ball of 10 mm diameter as the friction partner. All experiments were performed under a load of 1 N and a sliding speed of 0.073 m s^{-1} without lubrication at room temperature with a relative humidity of approximately 40%. In any testing program, three replicates should be included to certify the reliability of testing results. The friction coefficient curves were recorded continuously during the test process. The wear rate of the samples was calculated by measuring cross-sectional area of the wear scars with a surface profilometer (Form Talysurf PGI 1240, Taylor Hobson). The wear volume and wear rate of all coatings were calculated using equation (2) and (3), respectively.

$$V = \pi h d^2 / 8 \quad (2)$$

$$K = V / SF \quad (3)$$

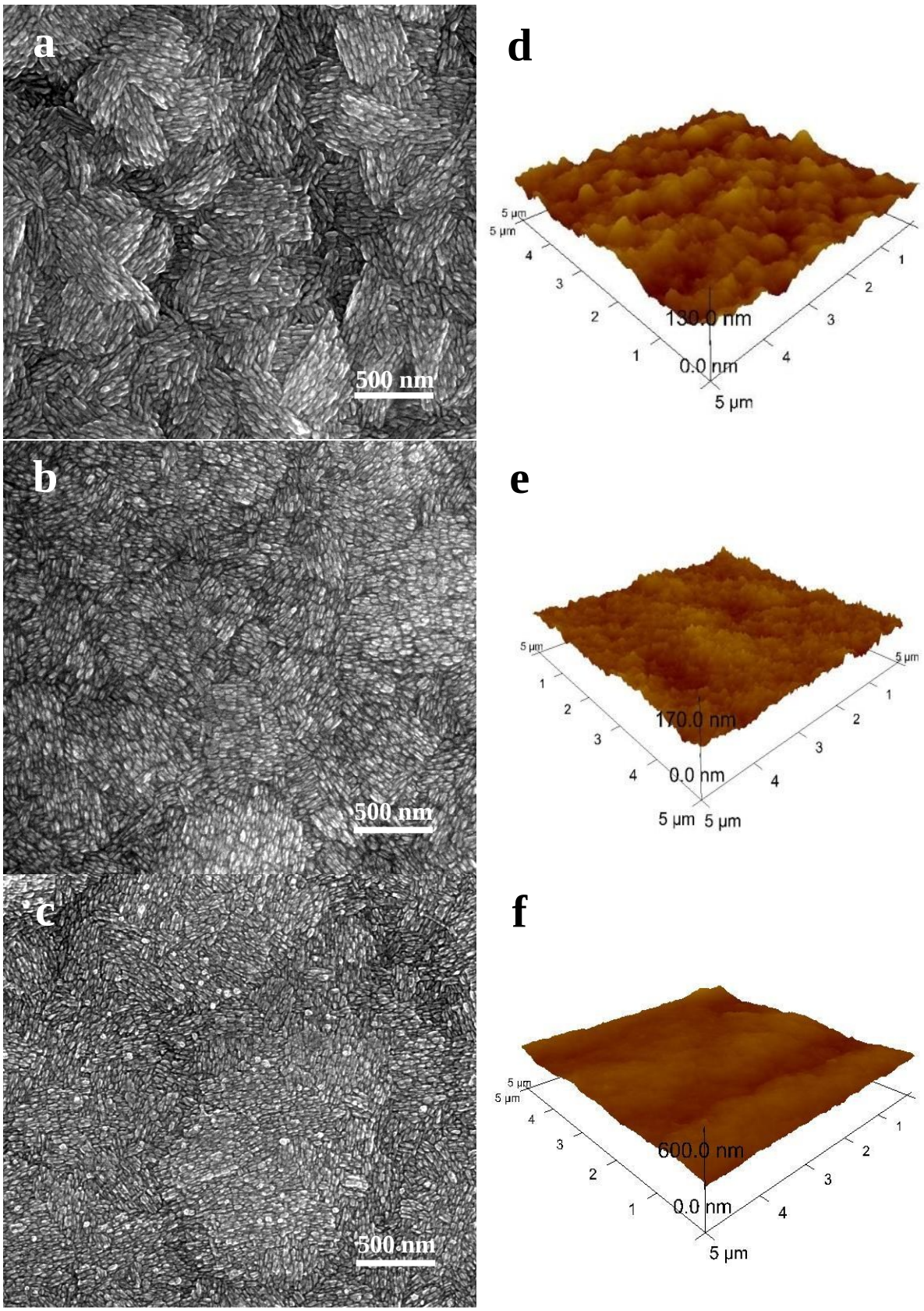

Fig. 1 FESEM and AFM images of nanocrystalline zinc coating deposited by (a,d) DC, (b,e) PC, and (c,f) PRC electrodeposition technologies.

Where K is the wear rate (in $mm^3\ Nm^{-1}$), V is the wear volume (in mm^3), h is the wear depth (in mm), d is the wear width (in mm), S is the total sliding distance (in m), and F is the normal load (in N).[25,26] After friction and wear tests, the surface morphology, element composition and load-displacement curve of the wear scars were analyzed by FESEM, EDS and nanoindentation.

Results and discussion

Influence of the current waveforms on electrodeposition of nanocrystalline zinc coatings

As we all know, the most commonly used current waveforms in electrodeposition techniques include direct current (DC), pulsed current (PC, the periodic pulse current with a pulse only in the positive direction.) and pulse reverse current (PRC, the periodic reverse pulse current with pulses in both the positive and negative direction.), which have considerable effects on the mechanism, morphology and current efficiency of electrodeposits.[27] Fig. 1 gives the FESEM and AFM morphologies of DC, PC and PRC electrodeposition of nanocrystalline zinc coatings from a basic sulfate bath ($ZnSO_4$•$7H_2O$ 100 g L^{-1} and H_3BO_3 20 g L^{-1}) containing polyacrylamide of 1 g L^{-1}. Surface morphology of DC, PC, and PRC electrodeposition of nanocrystalline zinc coatings examined by FESEM are illustrated in Fig. 1a, b and c, respectively. It can be seen that the nanocrystalline zinc coatings produced by different current waveforms show approximately spherical-shaped particles and the grain size is under 50 nm. Through comparison, it is found that the surface structure of PC and PRC electrodeposition of zinc coatings is more homogeneous, denser and finer than that of DC electrodeposition of zinc coating. Surface morphology characterized by AFM measurements also indicates that the nanocrystalline zinc coating obtained by the PRC electrodeposition is smoother relative to DC and PC electrodeposition, as shown in Fig. 1d, e and f.

Combination of FESEM and AFM results suggests that the DC electrodeposited coatings suffers the disadvantage of coating defects (surface roughness, porosity, undesirable microstructure, *etc.*) compared with the PC and PRC electrodeposited coatings. The PC electrodeposition has significant advantages in control of the grain size, surface morphology and preferred orientation of the coating than the DC electrodeposition. It can overcome these deficiencies of DC electrodeposition by the application of periodically alternating current. Many investigations have studied the viability of pulse current in PC electrodeposition for better controlling the structure and properties of nanocrystlline zinc coatings and have obtained similar results.[28-30] The difference in morphology and structure between PC and PRC electrodeposition can be attributed to the reason that the PRC electrodeposition can significantly improve the thickness distribution, and eliminate hydrogen embrittlement as well as leave the surface of the coating in an activated state by the application of periodically alternating current between positive and negative values (The schematic view of PRC vs. time curve is shown in Fig. 2.). Therefore, the PRC electrodeposition can produce smoother, denser, lower porosity and better adhesion coatings. Moreover, the anodic dissolution effect of the reverse current also makes the Zn^{2+} concentrations of cathode surface rise rapidly, which is favorable for using higher pulse current density in later cathode cycle. The high pulse current density heightens nucleation rate much more than the growth rate of the coating, and thus, it produces a coating with a finer grain size. Therefore, zinc coatings produced by PRC electrodeposition have better smoothing ability than the coatings prepared through PC electrodeposition, which fabricated similar coatings in the bath without any additives to the bright coatings prepared by DC electrodeposition in the bath with additives.[31-35]

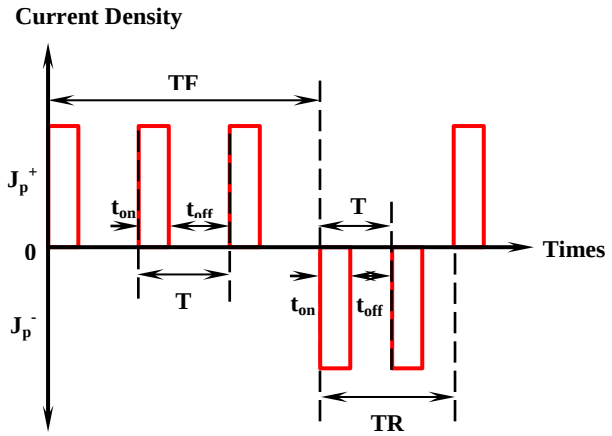

Fig. 2 Schematic diagram of the pulse reverse current technique.

XRD patterns obtained from nanocrystalline zinc coatings electrodeposited by DC, PC and PRC methods are illustrated in Fig. 3. The corresponding average grain sizes of the coatings calculated by Scherrer's formula are summarized in Table 2. As seen from Fig. 3, all XRD patterns show the three major diffraction peaks of zinc (100), (101) and (110) associated with a hexagonal structure that represents the crystallographic orientation of zinc. The diffraction peak intensity corresponding to the (110) plane is larger than the other peaks, indicating that the coatings have a well preferred orientation along the (110) direction, and the current waveforms have no influence on the crystallographic orientation. The calculated results of grain size inferred that pulse electrodeposition (PC and PRC) methods can

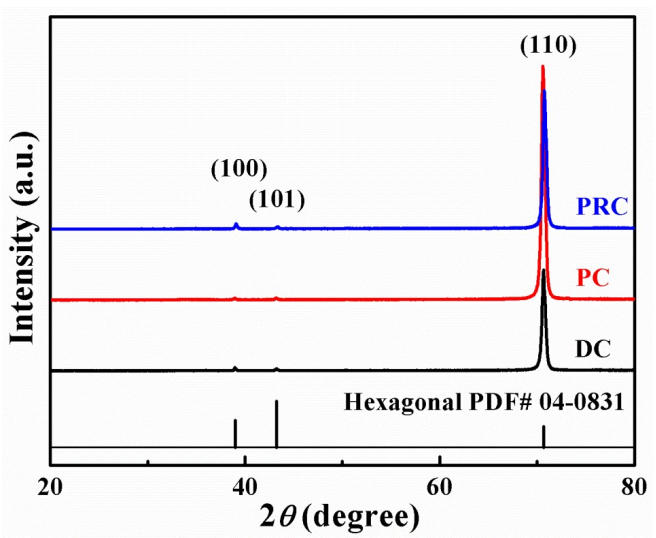

Fig. 3 XRD patterns from nanocrystalline zinc coatings deposited by DC, PC and PRC electrodeposition technologies.

reduce the grain size of the coatings more obviously than DC electrodeposition, which are in reasonable agreement with the FESEM observed results. For the coatings prepared by DC, PC and PRC techniques, similar results were obtained by Nasirpouri *et al.*[27] for the electrodeposition of nanocrystalline nickel in Watts bath.

Table 2 The calculated grain size through XRD patterns.

Current waveform	Grain size (nm)			
	Peak/2θ			Average
	(100) 38.99 °	(101) 43.22 °	(110) 70.63 °	
DC	56.2	38.5	22.7	39.13
PC	24.4	22.6	21.9	22.97
PRC	23.8	19.6	21.5	21.63

As mentioned above, the PRC electrodeposition not only kept the advantages of PC electrodeposition but also improved the performance of levelling off the coatings, so PRC electrodeposition has a dual role in both smoothing and grain refinement of the coatings compared to DC electrodeposition. A large number of studies have indicated that the grain size and surface roughness have a significant effect on the hardness and the friction coefficient of coatings. In general, the microhardness of coatings increased with decreasing grain size.[14-16] And the smoother the coating is, the better the wear resistance ability is, when the hardness of the coating is the same.[17,36] Hence, it can be concluded that PRC electrodeposition of nanocrystalline zinc coating has obvious advantages in improving the friction and wear property of the coating than DC and PC electrodeposition.

Surface morphologies and friction coefficients of zinc coatings

The surface morphologies of coarse-grained and nanocrystalline zinc coatings are shown in Fig. 4. Both of the FESEM micrographs are electrodeposited by PRC technique. It can be seen that the FESEM micrograph of the coating obtained from the basic sulfate bath shows an irregular coarse-grained size. In the additive-free sulfate bath, the coating displays the hexagonal zinc plates aligned parallel to the substrate, which indicating that the hexagonal structure of zinc is preserved in the zinc electrodeposition. By comparing with the coarse-grain zinc coating, the FESEM micrograph of the nanocrystalline zinc coating obtained from the optimum bath shows a uniform, dense and fine surface structure.

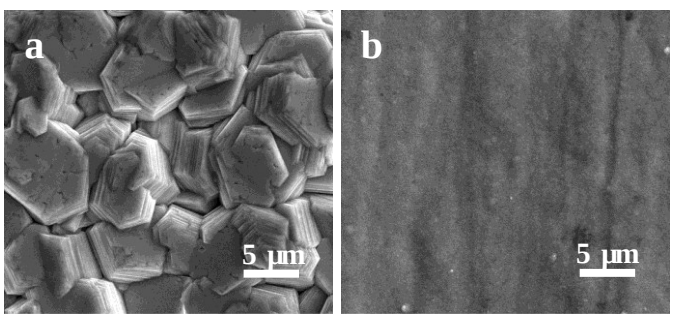

Fig. 4 Surface morphologies of the coarse-grained (a) and nanocrystalline (b) zinc coatings.

The variation curves of friction coefficients with the sliding duration on the surface of coarse-grained and nanocrystalline zinc coatings are illustrated in Fig. 5. It can be noticed that both of the friction coefficients increase from a low value to a very high value within the running-in period thereafter, friction coefficient marginally decreases and attains a steady-state value with the extending of sliding time. For coarse-grained zinc coating, the friction coefficient varies in the range 0.6-0.8, accompanied by severe oscillation. Compared with the coarse-grained zinc coating, the friction coefficients of nanocrystalline zinc coating are much more stable, and show a lower vibration. Hence, it can be concluded that the nanocrystalline zinc coating exhibits excellent friction reduction effect than the coarse-grained zinc under the same wear conditions.

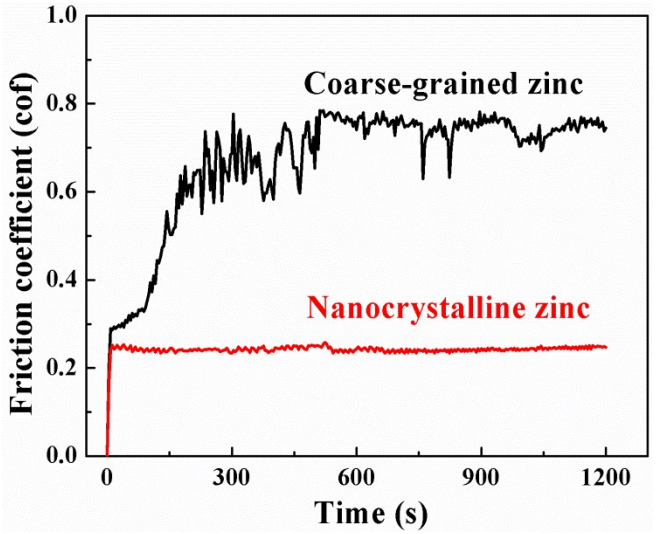

Fig. 5 Friction coefficient curves of the coarse-grained and nanocrystalline zinc coatings.

Cross-sectional morphologies and nanohardness of zinc coatings

The cross-sectional morphologies of coarse-grained and nanocrystalline zinc coatings produced under the same electrodeposition parameters are shown in Fig. 6. The images display that both coatings have firm adherence to the substrate and almost no defect in the deposited regions. For the coarse-grained zinc coating, the thickness is about 16 μm and the coating with a rough surface has a non-uniform thickness distribution. Compared with the coarse-grained zinc coating, the thickness of nanocrystalline zinc coatings is approximately 12 μm with a relatively smoother surface and more uniform thickness distribution. The thickness decrease of nanocrystalline zinc coating can be attributed to the fact that the

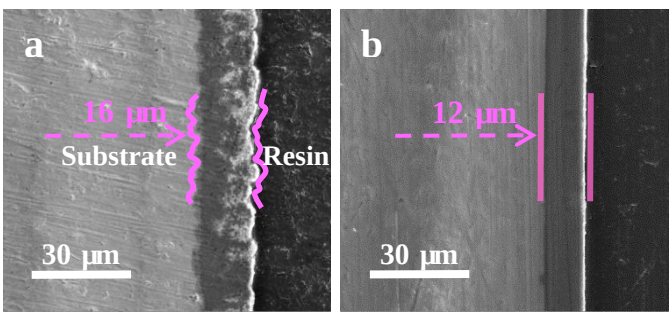

Fig. 6 Cross-sectional morphologies of the coarse-grained (a) and nanocrystalline (b) zinc coatings.

absorption of the polyacrylamide on the surface of the electrode suppresses the propagation of the reagent particles and decreases the concentration of the reactive ions, thereby increases the overpotential of the cathode as well as decreases the current efficiency.[15] Meanwhile, the increase of overpotential increases the free energy to form new nuclei and it results in a higher nucleation rate and finer grain size.[37]

The corresponding nanohardness distribution along the thickness direction is investigated through the nano-indentation technique. The typical load-displacement curves of different coatings are shown in Fig. 7. The maximum displacement results from elastic and plastic deformation, with elastic recovery occurring on unloading. The loads applied to reach the same penetration depth of 1000 nm are 16.8 and 48.3 mN for coarse-grained and nanocrystalline zinc coatings. In general, under a certain indentation depth, the bigger the maximum load is, the harder the material is. It can be seen that the nanohardness of nanocrystalline zinc coating is almost three times harder than that of the coarse-grained zinc. The hardness differences of the coatings could be explained by Hall-Petch law.[38, 39]

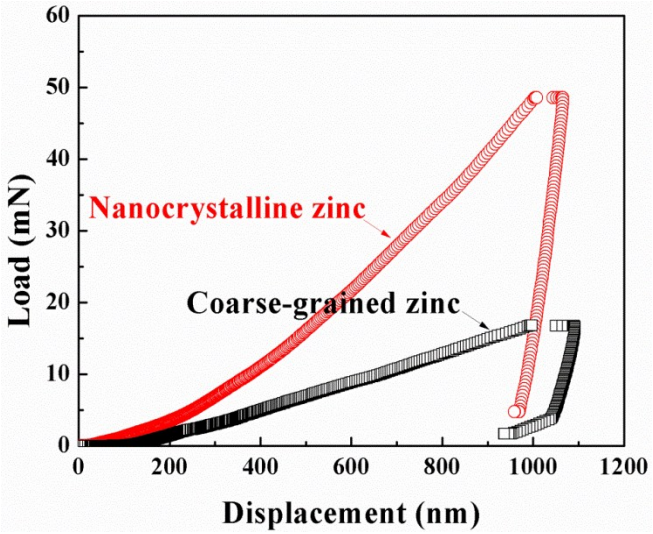

Fig. 7 Load-displacement curves of the coarse-grained and nanocrystalline zinc coatings.

Volume wear rate of zinc coatings

The cross-sectional profiles of the worn scar made on coarse-grained and nanocrystalline zinc coatings after the test of friction coefficient for 600 s are shown in Fig. 8, which clearly determine the shape and the depth of wear track, and thus the wear volume. The reproducibility of the presented data was generally checked by using 3 replicates, and typical results are reported. It can be seen that the wear depth of the nanocrystalline zinc coating is approximate 1.2 μm, which is within the nanocrystalline layer (12 μm thickness), while the wear depth is about 9.1 μm (the average thickness of coating is 16 μm) for the coarse-grained zinc coating under the same experimental conditions. The wear width of nanocrystalline zinc coating is also less than that of coarse-grained zinc coating. A summary of the volume abrasion rate (K) derived from the profile curve of worn scar (calculated from the wear scar profiles of three replicates) is also listed in Table 3. The average $K_{average}$ of coarse-grained and nanocrystalline zinc coatings is 2.6582×10^{-5} and 1.1032×10^{-6} mm^3 Nm^{-1}, respectively. The $K_{average}$ of the nanocrystalline zinc coating is approximately 1/24 of that of the coarse-grained counterpart. Apparently, the reduction of grain size to nanocrystalline can improve the friction and wear property of coarse-grained zinc coating significantly.

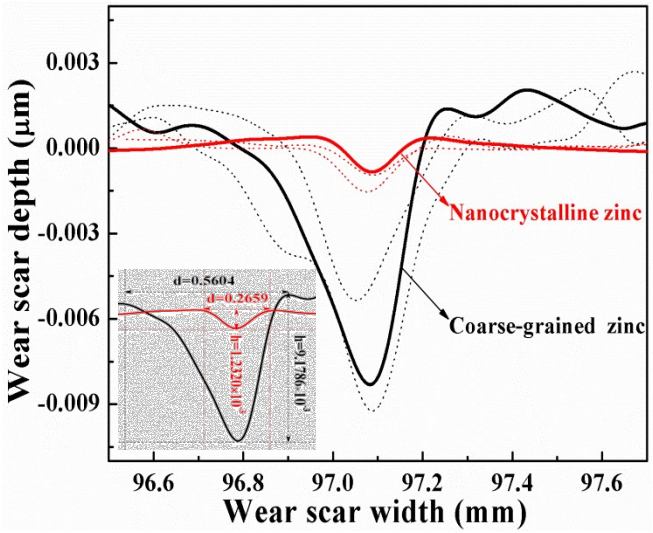

Fig. 8 Cross-sectional profiles of the worn scars made on coarse-grained and nanocrystalline zinc coatings.

Table 3 Volume wear rate K of coarse-grained (CG) and nanocrystalline (NC) zinc coatings after the test of friction and wear.

Sample	h	d	K	$K_{average}$
	mm	mm	mm^3 Nm^{-1}	mm^3 Nm^{-1}
CG	6.5356×10^{-3}	0.5277	1.6309×10^{-5}	2.6582×10^{-5}
	9.1786×10^{-3}	**0.5604**	**2.5831×10^{-5}**	
	9.5524×10^{-3}	0.6628	3.7605×10^{-5}	
NC	1.7493×10^{-3}	0.3394	1.8057×10^{-6}	1.1032×10^{-6}
	1.2320×10^{-3}	**0.2659**	**7.8057×10^{-7}**	
	0.9428×10^{-3}	0.2926	7.2333×10^{-7}	

Characteristics of worn scar surfaces

In order to further confirm the improvement in wear resistance, and investigate the tribolobical behavior for nanocrystalline zinc coating, the morphology and elemental composition of worn scar for coarse-grained and nanocrystalline zinc coatings after the test of friction coefficient for 600 s are shown in Fig. 9. It can be seen that the wear track of coarse-grained zinc coating (Fig. 9a) is characterized by typical features of adhesive and abrasive wear, with evident grooves and ploughs parallel to the sliding direction. The wear scar shows a larger extent of adhesion wear and severe plastic deformation, which results in the larger extent of coating delamination and increases the formation probability of asperity junctions. This explains that the coarse-grained zinc coating exhibits much higher vibration of friction coefficient and bigger fluctuation of wear track profile as shown in Figs. 5 and 8. Compared with the coarse-grained zinc coating, the nanocrystalline zinc coating exhibits the smaller width of wear grooves and negligible plastic deformation (Fig. 9b). Such change in morphology of worn scar is due to the reduction of grain size to nanocrystalline, which increases the hardness significantly and thereby reduces the

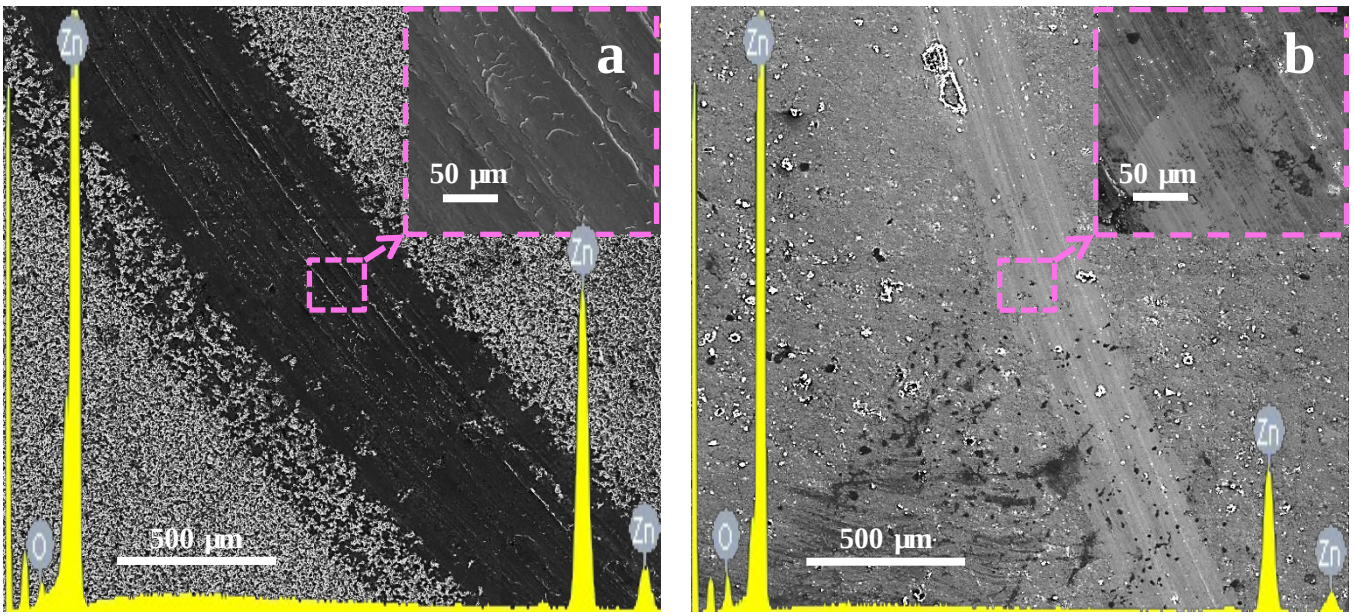

Fig. 9 FESEM morphologies and element compositions for the worn surfaces of coarse-grained (a) and nanocrystalline (b) zinc coatings after the test of friction and wear.

plastic deformation of nanocrystalline zinc coating. Moreover, the EDS analysis shows that the atomic oxygen content in the coarse-grained zinc coating is less than that in the nanocrystalline zinc coating. It is an indication that the nanocrystalline zinc coating shows an oxidation wear,[25] which can be attributed to the fact that the nanocrystalline zinc coatings are characterized by a high-volume fraction of grain boundary, so zinc atoms that are at the grain boundaries possess a higher activity and are prone to oxidation under the same friction and wear condition.

The load-displacement curve analysis is also carried out for worn scars of coarse-grained and nanocrystalline zinc coatings and the curves are shown in Fig. 10. In the case of the nanocrystalline zinc coating, the hardness of the coating does not show a clear change before and after the tribological test. As for coarse-grained zinc coating, the friction and wear behaviour leads to a significant reduction in the hardness of the coating. This case is caused by the truth that a considerable amount of zinc is redistributed over the surface in form of these wear debris and smeared by the repeated sliding action, therefore, an adhesive film is formed, whose hardness is lower than that of the coating itself. Through the comparison of load-displacement curves for coatings, wear scars and the substrate, the hardness of the substrate is higher than that of the coarse-grained zinc coating and lower than that of the nanocrystalline zinc coating before and after wear test. It implies that the friction and wear behaviour does not reach the substrate, and the result of nanoindentation measurement is reliable. From the above results, it is deduced that the friction and wear mechanism of zinc coatings experiences the transition from severe adhesion and abrasion wear to a slightly abrasion and oxidation wear with the reduction of grain size.

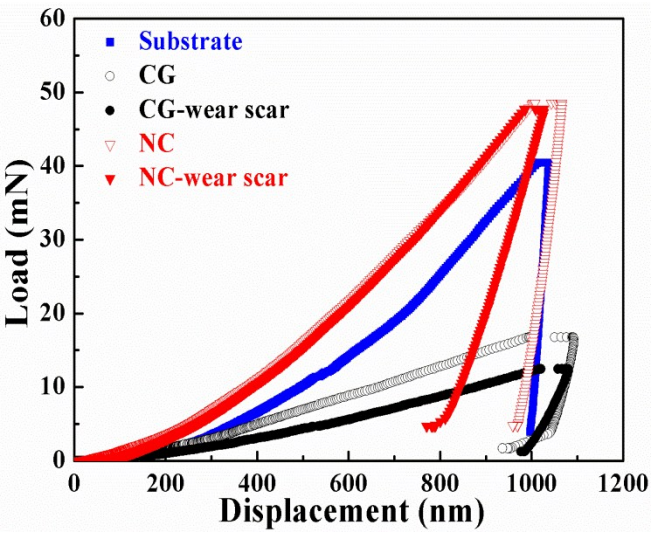

Fig. 10 Load-displacement curves for the worn surfaces of coarse-grained (CG) and nanocrystalline (NC) zinc coatings after the wear test.

Conclusion

The tribological behavior of zinc coatings changing with the reduction of grain size is described in this paper, which is to improve the friction and wear property of the conventional coarse-grained zinc coatings. The following main findings are resulted from the present investigation:

(1) Nanocrystalline zinc coatings produced by DC, PC and PRC electrodeposition consist of approximately spherical-shaped ultrafine crystallites in size ranging from 21 nm to about 39 nm, and have the (110) crystallographic preferred orientation. The positive periodically alternating currents of PC and PRC electrodeposition have significant advantages in control of the grain size distribution and surface morphology of the coating than DC electrodeposition. Moreover, the reverse periodically alternating currents of PRC electrodeposition can dissolve the particles with a larger grain size on the surface of coatings, which made the coatings smoother. Therefore, the

PRC electrodeposition of nanocrystalline zinc coating has apparent advantages in improving the hardness (according to the Hall-Petch law) and roughness of the coating than DC and PC electrodeposition.

(2) The variation of friction coefficients of the nanocrystalline zinc coating produced by PRC electrodeposition is much lower and more stable than that of the coarse-grained zinc coating. It indicates that the nanocrystalline zinc coating exhibited an excellent friction reduction effect. Moreover, the hardness of nanocrystalline zinc coating produced by PRC electrodeposition is almost three times that of the coarse-grained zinc. And, the average wear rate of the nanocrystalline zinc coating is approximately 1/24 of that of the coarse-grained zinc under the same friction and wear conditions. All above results have consistently shown that PRC electrodeposition of nanocrystalline zinc coating is an effective method to improve the friction and wear property of zinc coating.

(3) In summary, the friction and wear mechanism of zinc coatings experiences the transition from severe adhesion and abrasion wear (coarse-grained zinc) to a slightly abrasion and oxidation wear (nanocrystalline zinc) as a result of grain size reduction. The difference of tribological behavior between coarse-grain zinc and nanocrystalline zinc can be attributed to the increase of hardness, the decrease of surface roughness and the higher activity of zinc atoms at the grain boundaries with the reduction of grain size.

Notes and references

[a] State Key Laboratory of Urban Water Resource and Environment, School of Chemical Engineering and Technology, Harbin Institute of Technology, No. 92 West-Da Zhi Street, Harbin 150001, China. Tel: 86-451-86418616; E-mail: mzan@hit.edu.cn.

[b] Jiangsu Fasten Group, No. 165 Cheng-Jiang Zhong Street, Jiangyin 214434, China.

1 P. Skarpelos and J. W. Morris Jr, *Wear*, 1997, **212**, 165.
2 A.M. Alfantazi and U. Erb, *Corrosion*, 1996, **52**, 880.
3 K.M. Youssef, C.C. Koch and P.S. Fedkiw, *Corros. Sci.*, 2004, **46**, 51.
4 D.H. Jeong, F. Gonzalez, G. Palumbo, K.T. Aust and U. Erb, *Scripta Mater.*, 2001, **44**, 493.
5 Y.R. Jeng, P.C. Tsai and S.H. Chiang, *Wear*, 2013, **303**, 262.
6 K.H. Hou, H.H. Sheu and M.D. Ger, *Appl. Surf. Sci.*, 2014, **308**, 372.
7 M.R. Zamanzad-Ghavidel, K. Raeissi and A. Saatchi, *Mater. Lett.*, 2009, **63**, 1807.
8 L. Liu, Y. Li and F. Wang, *J. Mater. Sci. Technol.*, 2010, **26**, 1.
9 I. Matsui, T. Kawakatsu, Y. Takigawa, T. Uesugi and K. Higashi, *Mater. Lett.*, 2014, **116**, 71.
10 L. Lu, M.L. Sui and K. Lu, *Science*, 2000, **287**, 1463.
11 I. Matsui, H. Mori, T. Kawakatsu, Y. Takigawa, T. Uesugi, and K. Higashi, *Mater. Sci. Eng. A*, 2014, **607**, 505.
12 M. Hakamada, Y. Nakamoto, H. Matsumoto, H. Iwasakib, Y. Chena, H. Kusudaa and M. Mabuchi, *Mater. Sci. Eng. A*, 2007, **457**, 120.
13 L. Lu, Y. Shen, X. Chen, L. Qian and K. Lu, *Science*, 2004, **304**, 422.
14 C.N. Panagopoulos, K.G. Georgarakis and A. Anagnostopoulou, *Mater. Lett.*, 2006, **60**, 133.
15 K. Saber, C.C. Koch and P.S. Fedkiw, *Mater. Sci. Eng. A*, 2003, **341**, 174.
16 R. Mishra, B. Basu and R. Balasubramaniam, *Mater. Sci. Eng. A*, 2004, **373**, 370.
17 X.H. Wu, P.B. Su, Z.H. Jiang and S. Meng, *ACS appl. Mater. Inter.*, 2010, **2**, 808.
18 G. Meng, L. Zhang, Y. Shao, T. Zhang and F. Wang, *Corros. Sci.*, 2009, **51**, 1685.
19 M.C. Li, L.L. Jiang, W.Q. Zhang, Y.H. Qian, S.Z. Luo and J.N. Shen, *J. Solid State Electrochem.*, 2007, **11**, 1319.
20 R. Ramanauskas, L. Gudavičiūtė, R. Juškėnas and O. Ščit, *Electrochim. Acta*, 2007, **53**, 1801.
21 H.B. Muralidhara and Y. Arthoba Naik, *Surf. Coat. Technol.*, 2008, **202**, 3403.
22 H.B. Muralidhara and Y.A. Naik, *Bull. Mater. Sci.*, 2008, **31**, 585.
23 Q.Y. Li, Z.B. Feng, J.Q. Zhang, P.X. Yang, F.H. Li and M.Z. An, *RSC Adv.*, 2014, **4**, 52562.
24 B.D. Cullity, *Elements of X-ray Diffraction*, Addison Wesley Publishing Company, Inc., Philippines, 2nd edn, 1978, p. 284.
25 L.P. Wang, Y. Gao, T. Xu and Q.J. Xue, *Mater. Chem. Phys.*, 2006, **99**, 96.
26 B. Yin, H.D. Zhou, D.L. Yi, J.M. Chen and F.Y. Yan, *Surf. Eng.*, 2010, **26**, 469.
27 F. Nasirpouri, M.R. Sanaeian, A.S. Samardak, E.V. Sukovatitsina, A.V. Ognev, L.A. Chebotkevich, M.-G. Hosseini and M. Abdolmaleki, *Appl. Surf. Sci.*, 2014, **292**, 795.
28 K.M. Youssef, C.C. Koch and P.S. Fedkiw, *Electrochim. Acta*, 2008, **54**, 677.
29 M.S. Chandrasekar and P. Malathy, *Mater. Chem. Phys.*, 2010, **124**, 516.
30 M.S. Chandrasekar, S. Srinivasan and M. Pushpavanam, *J. Mater. Sci.*, 2010, **45**, 1160.
31 L. Chang, *J. Alloys Compd.*, 2008, **466**, L19.
32 K.M. Yin, *Surf. Coat. Technol.*, 1997, **88**, 162.
33 N.V. Mandich, *Met. Finish.*, 2000, **98**, 375.
34 M.S. Chandrasekar and M. Pushpavanam, *Electrochim. Acta*, 2008, **53**, 3313.
35 W. Cheng, W. Ge, Q. Yang and X.X. Qu, *Appl. Surf. Sci.*, 2013, **276**, 604.
36 S. Tao and D. Li, *Nanotechnology*, 2006, **17**, 65.
37 A. M. El-Sherik and U. Erb, *J. Mater. Sci.*, 1995, **30**, 5743.
38 E.O. Hall, *Proc. Physl. Soc. Sect. B*, 1951, **64**, 747.
39 N.J. Petch, *J. Iron. Steel. Inst.*, 1953, **174**, 25.

